

Enhancement of the Electrocatalytic Activity of Conducting Polymer/Pd Composites for Hydrazine Oxidation by Copolymerization

Shimaa M. Ali^{1,2,*}, Khadija M. Emran¹, Hamedh A. Al lehaibi¹

¹ Department of Chemistry, Faculty of Science, Taibah University, Madinah 30002, KSA

² Department of Chemistry, Faculty of Science, Cairo University, Giza 12613, Egypt

*E-mail: dr_shimaaali80@yahoo.com

Received: 27 April 2017 / Accepted: 23 July 2017 / Published: 13 August 2017

Poly(ANI-co-Py)/Pd composite was prepared by electrochemical polymerization from a mixed monomer solution in 0.5 M LiClO₄/acetonitrile. The prepared composite was investigated as a catalyst for the electrooxidation of hydrazine by cyclic voltammetry (CV) and electrochemical impedance spectroscopy (EIS). Scanning electron microscope (SEM) photos showed that Pd particles are uniformly distributed over the rough copolymer surface. The electrocatalytic activity of the prepared composite was compared with those of individual polymers composites, polyaniline/Pd (PANI/Pd) and polypyrrole/Pd (PPY/Pd). It was proved that the copolymerization enhanced the electrocatalytic activity toward hydrazine oxidation as indicated by the increased oxidation peak current in CV and the reduced charge transfer resistance determined by EIS. The optimum pH for performing the hydrazine oxidation by the proposed catalyst is 6. Kinetic study shows that the process is diffusion-controlled with a diffusion coefficient value of $1.94 \times 10^{-4} \text{ cm}^2 \cdot \text{s}^{-1}$. A linear calibration curve was obtained between 3 mM and 0.01 M with a sensitivity value of $98.31 \mu\text{A} \cdot \text{mM}^{-1}$ and a limit of detection (LOD) value of 0.38 μM . The presented composite showed good stability, reproducibility, and selectivity for hydrazine oxidation.

Keywords: conducting polymers; palladium-based sensor; composite; hydrazine oxidation.

1. INTRODUCTION

Since the discovery of stable conjugated conducting polymers (CPs) in 1977, such as polyaniline (PANI), polypyrrole (PPY), and polythiophene (PT), studies on CPs have been greatly promoted due to their unique properties, such as good electronic and optical properties, conductivity that can reach values of 10^3 S/cm upon doping, flexible mechanical properties, ease of processing, and attractive electrochemical redox activity which facilitates its applications in many electrochemical devices [1,2]. Composites of CPs can be prepared by introducing a secondary inorganic/organic

component which is biologically active to a given species, thus, expanding CP applications to catalytic and sensing purposes. CPs/Pd composites can be prepared by the chemical/electrochemical reduction of a Pd salt in the presence of the CP as a matrix for Pd particles. These composites attracted the interest of many researchers as it offered enhanced catalytic properties due to the dispersion of metallic particles through the polymeric matrix, resulting in a larger reaction surface area [3]. CPs/Pd composites were found to be selective and good catalysts for hydrogenation and oxidation reactions of organic compounds [4–8]. In addition, they can exhibit improved and sensitive responses to small concentrations, this high-sensing ability raised from their high charge transfer properties and strong covalent bonds formed between polymeric functional groups and biological compounds. Several CPs/Pd composites have been also reported as chemical and biochemical sensors for many important compounds in environmental and health applications [9–12]. Recently, Sener et al. have reported that the sensing properties of CPs toward glucose can be highly enhanced by copolymerization [13], where the palladium complex of 3,4-ethylenedioxythiophene can be copolymerized with 4-amino-N-(2,5-di(thiophene-2-yl)-1H-pyrrol-1-yl)benzamide to provide an amperometric glucose sensor based on glucose oxidase. This enhancement is due to the synergism of the enzyme immobilization by the amino groups of 4-amino-N-(2,5-di(thiophene-2-yl)-1H-pyrrol-1-yl)benzamide and, at the same time, the improved charge mediation of the bio-electrocatalytic reaction offered by the palladium complex of 3,4-ethylenedioxythiophene.

Hydrazine detection is very important as it is widely used as a raw material in many agricultural chemicals. Hydrazine is also a commonly used fuel in fuel cells, particularly direct hydrazine fuel cells, due to its high hydrogen content. However, it is highly toxic and can be harmful to the nervous system upon continuous exposure [14–16]. Several Pd-based sensors have been employed for the electrooxidation of hydrazine, such as carbon-supported Pd nanoparticles [17], Pd/carbon nanotube composites [18], Pd/carbon nanotube/Nafion composite [19], and Pd/Au supported on amino-functionalized TiO₂ nanotubes [20]. Examples of CP-based hydrazine sensors are PPY/lignosulfonate and polyethylenedioxythiophene/lignosulfonate composites [21], PANI/Ni-porphyrin catalyst [22] and, recently, PANI/Pd multilayered catalyst proposed by Liu et al. [23].

In this work, a copolymer of aniline (ANI) and pyrrole (PY) composite with Pd, poly(ANI-co-PY)/Pd composite, will be prepared by the electrochemical technique. The composite will be employed as a catalyst for the electrochemical oxidation of hydrazine, its response will be compared with those of PANI/Pd and PPY/Pd to show the enhancement caused by the copolymerization. Several factors affecting the sensor response, such as pH, scan rate, and interferences, will be studied. A calibration curve will be constructed to determine the low limit of detection (LOD) and the sensor sensitivity. In addition, the sensor reproducibility, selectivity, and stability will be investigated.

2. EXPERIMENTAL

2.1. Chemicals

All chemicals were used as received: PdCl₂ (99%), aniline (99.5%), pyrrole (99%), hydrazine (98%), HCl (37%), KCl, K₂HPO₄, KH₂PO₄, (NH₄)₂SO₄, and NaNO₃ (Sigma-Aldrich company). Doubly-distilled water was used for aqueous solution preparation.

2.2. Electrochemical Cell and Electrochemical Measurements

Electrochemical experiments were performed in a three electrode-one compartment glass cell. The working electrode was a glassy carbon (GC) disc (diameter = 1.6 mm), the counter electrode was a platinum wire, and all potentials are referenced to a 3 M Ag/AgCl electrode.

Electrochemical measurements were performed by a Gamry Interface 1000 unit. The polymer synthesis was carried out by repeated cyclic voltammetry in the monomer solution from -0.2 to 1.8 V at a scan rate of $100 \text{ mV}\cdot\text{s}^{-1}$. Pd catalyst deposition was done by applying a double potential step to the polymer film as follows: $E_1 = 0$ V for 30 s and $E_2 = +0.1$ V for 600 s [6]. The electrocatalytic oxidation of hydrazine was investigated by cyclic voltammetry from -0.5 to $+0.5$ V at a scan rate of $50 \text{ mV}\cdot\text{s}^{-1}$. Electrochemical impedance spectroscopy was recorded from 0.1 Hz to 100 kHz with an amplitude of 5 mV at a potential of 0 V.

2.3. Preparation of the Poly(ANI-co-PY)/Pd Sensor

Poly(ANI-co-PY)/Pd was deposited on the GC electrode by repeated cyclic voltammetry (three cycles) from a mixed solution of equal volumes of 0.025 M aniline and 0.05 M pyrrole, both prepared in 0.05 M LiClO₄/acetonitrile solutions. Then Pd was deposited from a 10^{-3} M PdCl₂/0.1 M HCl solution by a double potential step as mentioned above.

2.4. Surface Characterization

The surface morphology and analysis were investigated by using a scanning electron microscope (SEM)-energy dispersive X-ray (EDX) combined system (Superscan SS-550, Shimadzu, Japan).

3. RESULTS AND DISCUSSION

3.1. Effect of the Catalyst Substrate Type

To investigate the effect of the copolymerization on the catalytic properties of CPs/Pd composites, the cyclic voltammograms of GC/Pd, GC/PANI/Pd, GC/PPY/Pd, and GG/poly(ANI-co-PY)/Pd in 5 mM hydrazine/phosphate buffer solution (pH = 7), at a scan rate of $50 \text{ mV}\cdot\text{s}^{-1}$, are recorded, as shown in Figure 1. The inset represents the cyclic voltammograms of the same four cases in the blank solution. Before recording the cyclic voltammograms, electrodes were stirred in the test solution for 5 min to allow the system to reach a stable state [24].

It can be shown that the presence of a polymeric substrate enhances the electrocatalytic activity of the Pd catalyst toward hydrazine oxidation as indicated by the increase in the oxidation peak current (I_p), where an I_p value of GC/Pd, $93.8 \mu\text{A}\cdot\text{cm}^{-2}$, is increased to 124.2 and $149.8 \mu\text{A}\cdot\text{cm}^{-2}$ by introducing PANI and PPY substrates, respectively. Upon employing the poly(ANI-co-PY) substrate with the Pd

catalyst, GC/poly(ANI-co-PY)/Pd, the I_p value reaches the highest value of $204.8 \mu\text{A}\cdot\text{cm}^{-2}$. The dashed line in Figure 1 represents the response of GC/poly(ANI-co-PY) to the hydrazine oxidation, and it is clear that the copolymer itself has no catalytic performance, but rather enhances that of the Pd catalyst due to the enhanced charge mediation offered in the presence of the polymeric substrate. The peaks mentioned above for the four cases disappear in the blank solution, as shown in the inset in Figure 1, which indicates that all of these peaks are associated with the hydrazine oxidation.

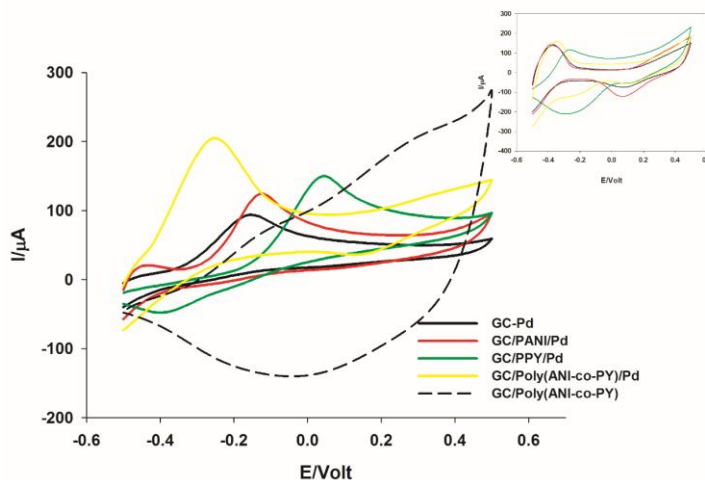
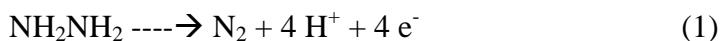


Figure 1. Cyclic voltammograms of different based-Pd catalysts in 5 mM hydrazine/phosphate buffer solution (pH = 7), a scan rate of $50 \text{ mV}\cdot\text{s}^{-1}$. The inset represents the response of different catalysts in the buffer.

3.2. Effect of pH

Figure 2 shows the pH effect on the electrocatalytic activity of poly(ANI-co-PY)/Pd for the hydrazine oxidation. Cyclic voltammograms at different pH values are performed in 5 mM hydrazine/phosphate buffer solution (pH ranges from 4–10) and a scan rate of $50 \text{ mV}\cdot\text{s}^{-1}$. It can be shown that the oxidation peak current increases from pH 4 to 6, then decreases at pH = 7. At higher pH values, there is no distinct peak for hydrazine oxidation, possibly due to retarded kinetics at higher pH values. The pKa value for hydrazine is 7.9 [25]. Therefore, the optimum pH value for the proposed sensor performance is 6 ($I_p = 347.4 \mu\text{A}\cdot\text{cm}^{-2}$). It can also be noticed that the peak potential for hydrazine oxidation (E_p) shifts to more negative value with increasing pH. A slope of $-65.4 \text{ mV}\cdot\text{pH}^{-1}$ is obtained by plotting the peak potential of the hydrazine oxidation vs. pH of the solution (figure not shown), which is close to the theoretical Nernstian slope ($-59 \text{ mV}\cdot\text{pH}^{-1}$), suggesting that the hydrazine oxidation includes an equal number of electrons and protons in the transfer process (four electrons–four protons transfer process) [26, 27] as shown in the following equation:



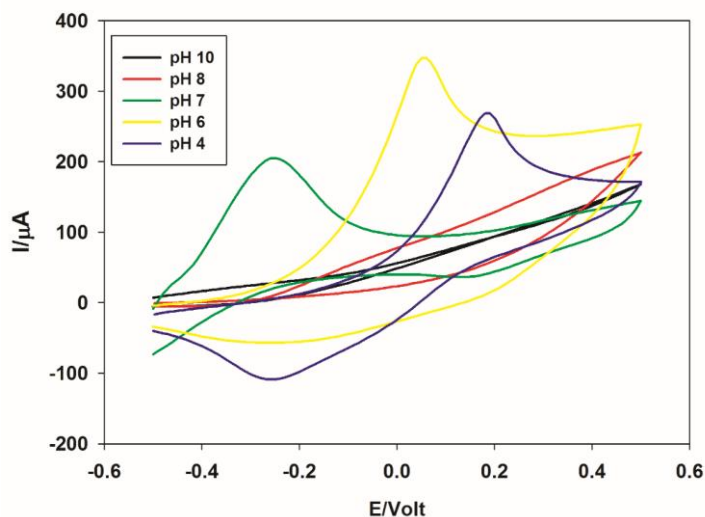


Figure 2. Cyclic voltammograms of GC/poly(ANI-co-PY)/Pd in 5 mM hydrazine/phosphate buffer solutions at different pH values, at a scan rate of $50 \text{ mV}\cdot\text{s}^{-1}$.

3.3. Effect of Scan Rate

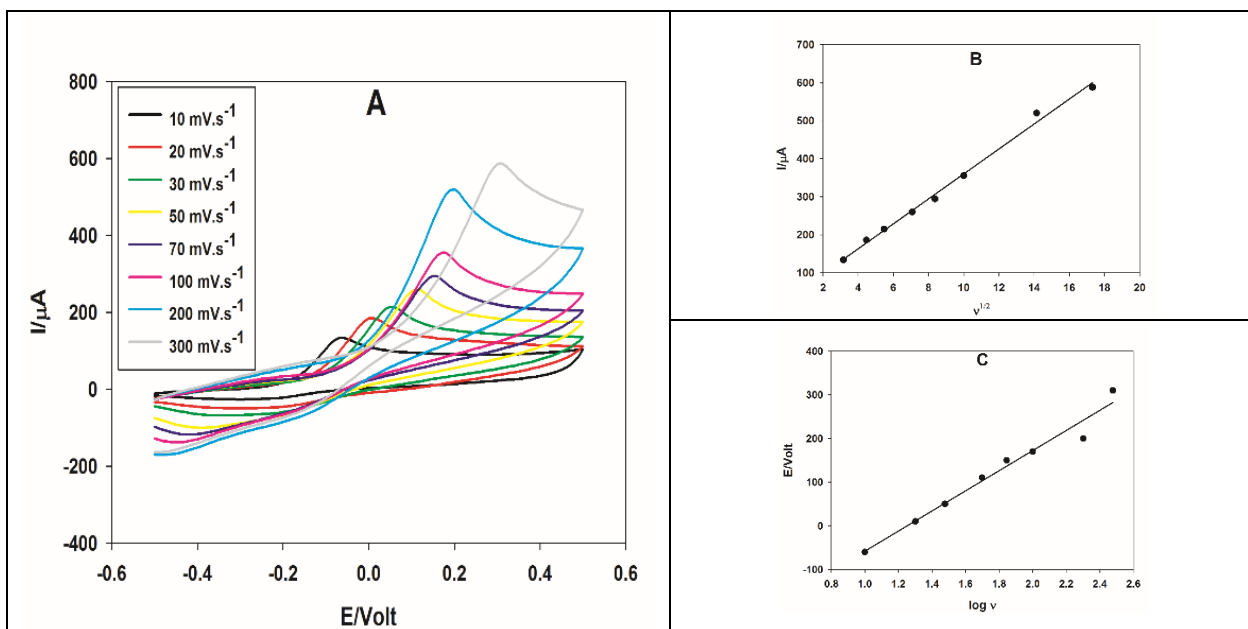


Figure 3. (A) Cyclic voltammograms of GC/poly(ANI-co-PY)/Pd in 5 mM hydrazine/phosphate buffer solutions at pH = 6 at different scan rates of 10–300 $\text{mV}\cdot\text{s}^{-1}$; (B) a plot of I_p vs. $v^{1/2}$; and (C) a plot of E_p vs. $\log v$.

The dependence of the electrocatalytic activity of the presented sensor on the scan rate of the cyclic voltammetric measurement was investigated. Figure 3A shows the cyclic voltammograms of GC/poly(ANI-co-PY)/Pd in 5 mM hydrazine/phosphate buffer solution (pH = 6) at different scan rates, ranging from 10 to 300 $\text{mV}\cdot\text{s}^{-1}$. It can be shown that the hydrazine oxidation peak potential (E_p) shifts

to a more positive value by increasing the scan rate, which indicates a kinetically-limited hydrazine oxidation on the presented sensor. In addition, the peak current (I_p) is linearly proportional to the square root of the scan rate ($v^{1/2}$), suggesting a diffusion-controlled process, as shown in Figure 3B. A plot of E_p vs. $\log v$ is found to be linear which indicates irreversible hydrazine oxidation, as shown in Figure 3C [21, 28].

In addition, Tafel slope (b) can be obtained by the following equation [20]:

$$E_p = \frac{b}{2} \log v + \text{Constant} \quad (2)$$

$$b = \frac{0.059}{(1-\alpha)n_\alpha} \quad (3)$$

where α is the transfer coefficient and n_α is the number of electrons participating in the rate determining step.

The value of (b) in this study was found to be 0.461 V/decade, by assuming that n_α is 1, as reported in several studies [20, 21, 28], and the value of α is 0.87.

The value of the diffusion coefficient (D) can be calculated from the following equation for the irreversible diffusion-controlled reaction [29]:

$$I_p = 3.01 \times 10^5 n [(1-\alpha)n_\alpha]^{1/2} ACD^{1/2} v^{1/2} \quad (4)$$

The calculated value of (D) is $1.94 \times 10^{-4} \text{ cm}^2 \cdot \text{s}^{-1}$.

3.4. Effect of Hydrazine Concentration

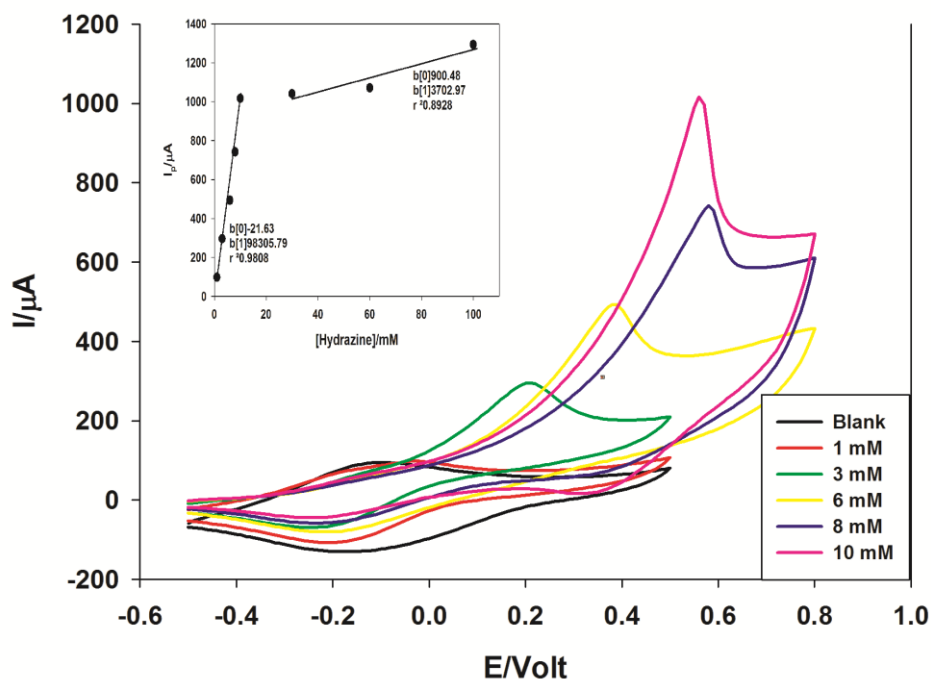


Figure 4. Cyclic voltammograms of GC/poly(ANI-co-PY)/Pd in the absence and presence of different hydrazine concentrations, 1 mM to 0.1 M, in phosphate buffer at pH = 6, a scan rate of $50 \text{ mV} \cdot \text{s}^{-1}$. The inset represents the calibration curve.

The electrocatalytic activity of poly(ANI-co-PY)/Pd toward hydrazine oxidation is examined in the absence and presence of different hydrazine concentrations in phosphate buffer (pH = 6), at a scan rate of $50 \text{ mV}\cdot\text{s}^{-1}$, as shown in Figure 4. The oxidation peak starts to appear at a hydrazine concentration of 3 mM at an oxidation potential of 0.21 V. A further increase in the hydrazine concentration (studied range = 1 mM to 0.1 M) results in a current increase due to oxidation with a shift in the oxidation potential to more positive values, as seen in Figure 4. The inset represents the calibration curve. Two linear ranges exist, 3 mM–0.01 M and 0.03 M–0.1 M with sensitivity values of 98.31 and $3.70 \mu\text{A}\cdot\text{mM}^{-1}$, respectively.

The limit of detection (LOD) of the proposed sensor for hydrazine can be calculated according to the following equation [30]:

$$\text{LOD} = 3 \text{ SD/slope} \quad (5)$$

where SD is the standard deviation of the blank (SD = 0.013) and the slope is that of the calibration curve. The LOD value for this sensor is $0.38 \mu\text{M}$.

Table 1. Comparison of poly(ANI-co-PY)/Pd sensor with other Pd-based sensors reported in literature for hydrazine electrooxidation.

Sensor	Linear range/ μM	Detection limit/ μM	Reference
Pd/PANI-doped polysulfonic acid	40×10^3	0.42	[31]
Pd/PANI nanoparticles	10-800	0.06	[32]
Pd/PANI nanoparticles multilayer	$0.2-12 \times 10^3$	0.05	[3]
Pd/MWCNTs/PPY nanoparticles	$0.1-5 \times 10^3$	0.04	[33]
Pd/Carbon black nanoparticles	$5-5 \times 10^4$	8.8	[34]
Pd/carbon nanoparticles	0.02-71	0.02	[35]
Pd/carbon nanofibers	$10-4 \times 10^3$	2.9	[36]
Pd nanowires/carbon ionic liquid	5-800	0.82	[37]
Pd nanoparticles/MWCNTs	0.1-10	0.016	[38]
Pd/carbon/CNTs	2-500	0.6	[39]
Pd/CNTs/Nafion	200-2500	8	[12]
Pd/Au nanoparticles/amino functionalized TiO_2	0.06-700	0.012	[20]
Pd/Au nanorod alloy	0.01-501	0.02	[40]
Pd/poly(ANI-co-PY)	10^4-10^5	0.38	This work

A comparison of Pd/poly(ANI-co-PY) with comparable sensors, Pd/CPs or Pd/carbon composites, reported in the literature is shown in Table 1. It can be seen that, although most of sensors mentioned in Table 1, are nanomaterials, the presented sensor still has a relatively low detection limit.

It is recommended, for future study, to prepare the Pd/conducting copolymer at the nanoscale to enhance its performance.

A simple and accurate standard method for hydrazine determination can be achieved by spectrophotometry, visible absorption at 455 nm [41]. In this method, hydrazine reacts with *p*-dimethylaminobenzaldehyde to form a yellow complex. The intensity of the complex color is directly proportional to the hydrazine concentration. The performance of the presented sensor for hydrazine determination is compared with the above mentioned standard method by using 5 mM of hydrazine solution. Upon hydrazine determination by the standard spectrophotometric method, the obtained hydrazine concentration is 4.15 mM while, by applying the proposed sensor electrochemically for hydrazine determination, the obtained concentration is 3.5 mM.

3.5. Stability, Reproducibility, and Selectivity

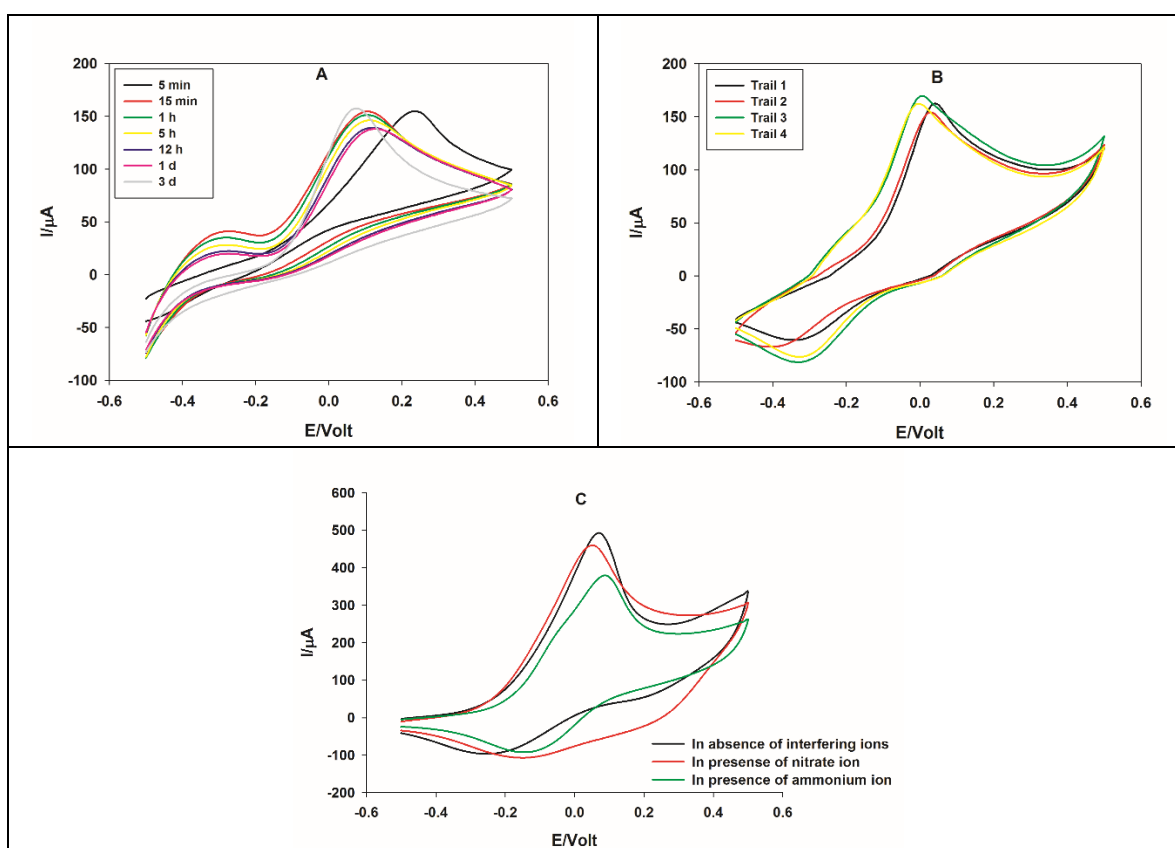


Figure 5. Cyclic voltammograms of GC/poly(ANI-co-PY)/Pd in 5 mM hydrazine/phosphate buffer at pH = 6, a scan rate of $50 \text{ mV}\cdot\text{s}^{-1}$, (A) at different test times, (B) using freshly prepared sensor each time before testing, and (C) in the absence and presence of interfering ions, and nitrate and ammonium ions.

The stability of the proposed GC/poly(ANI-co-PY)/Pd sensor is examined by performing the cyclic voltammograms in 5 mM hydrazine/phosphate buffer solution (pH = 6) and a scan rate of $50 \text{ mV}\cdot\text{s}^{-1}$, over a time period extended from 5 min to three days, as shown in Figure 5A. It is clear that the current due to the hydrazine oxidation is almost unchanged (the decrease in I_p is less than $20 \mu\text{A}$).

It is worth mentioning that the oxidation potential is 0.230 V upon performing CV after 5 min, then it shifts negatively to about 0.1 V at longer test times. Finally, after three days, the oxidation potential become 0.07 V. Therefore, in addition to the high stability of the sensor, the oxidation of hydrazine on it becomes easier with time, as indicated by the negative shift in the oxidation potential.

The reproducibility is checked by performing cyclic voltammograms of four freshly prepared sensor each time before testing in 5 mM hydrazine/phosphate buffer solution (pH = 6) and at a scan rate of $50 \text{ mV}\cdot\text{s}^{-1}$, as shown in Figure 5B. The value of the standard deviation of four oxidation peak currents is 3.06%, reflecting acceptable reproducibility of the poly(ANI-co-PY)/Pd sensor for hydrazine oxidation.

The selectivity of the presented sensor is investigated by performing the cyclic voltammograms in 5 mM hydrazine/phosphate buffer solution (pH = 6) and a scan rate of $50 \text{ mV}\cdot\text{s}^{-1}$, in the absence and presence of interfering species, such as NH_4^+ and NO_3^- , as shown in Figure 5C. The values of the oxidation peak current decrease to 85% and 70% of its value in the absence of any interferences, for nitrate and ammonium ions, respectively.

3.6. Electrochemical Impedance Spectroscopy

To probe the features of surface-modified electrodes, impedance spectroscopy is an effective technique. The electrochemical activity of GC/Pd and GC/poly(ANI-co-PY)/Pd in 5 mM hydrazine/phosphate buffer at pH = 6 has been examined. From the shape of Z'' vs. Z' impedance spectra presented in Figure 6, the electron-transfer kinetics and diffusion characteristics can be extracted according to the circuit model with the circuit description code (CDC) $R_s(Q_{f/s}[R_{f/s}(Z_w(R_{m/f}Q_{m/f}))])$ [38].

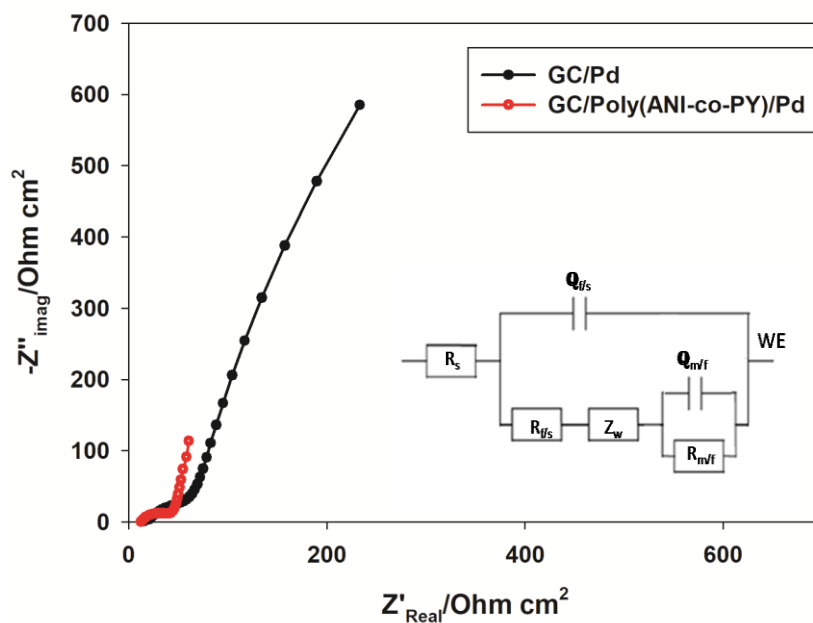


Figure 6. Nyquist plots in 5 mM hydrazine/phosphate buffer at pH = 6 for GC/Pd and GC/poly(ANI-co-PY)/Pd electrodes, for comparison.

The respective semicircle parameters correspond to the electron-transfer resistance (R_{ct}) and the double-layer capacity (C_{dl}) of the modified electrode, in Figure 6, show a smaller depressed semicircle arc ($R_{ct} = 63.6 (Z'/\Omega \text{ cm}^2)$) for the poly(ANI-co-PY)/Pd-modified GC electrode compared to the Pd-modified GC electrode ($R_{ct} = 814.0 (Z'/\Omega \text{ cm}^2)$). This lower electron-transfer resistance behavior represents the characteristics of the diffusion-limited electron-transfer process of the outer electrode surface of poly(ANI-co-PY)/Pd-modified GC electrode and reflecting the higher catalytic activity of the latter with respect to the Pd-modified GC electrode for hydrazine oxidation.

3.7. Surface Characterization of Copolymer/Pd Composite by Scanning Electron Microscope (SEM)

Figure 7 shows SEM images, with different magnifications at 2000 \times and 5000 \times (Figures 7A,B), and the energy dispersive X-ray analysis (EDXA) of the poly(ANI-co-PY)/Pd composite (Figure 7C). The surface of the composite is rough and composed of a dark background, representing the copolymeric matrix and the shiny spots of the Pd grains. It can be shown that Pd is uniformly distributed over the copolymer surface, providing a large surface area upon which the hydrazine oxidation can occur. The successful modification of the copolymer with Pd is further confirmed by the presence of Pd peaks in the EDXA spectrum (Figure 7C).

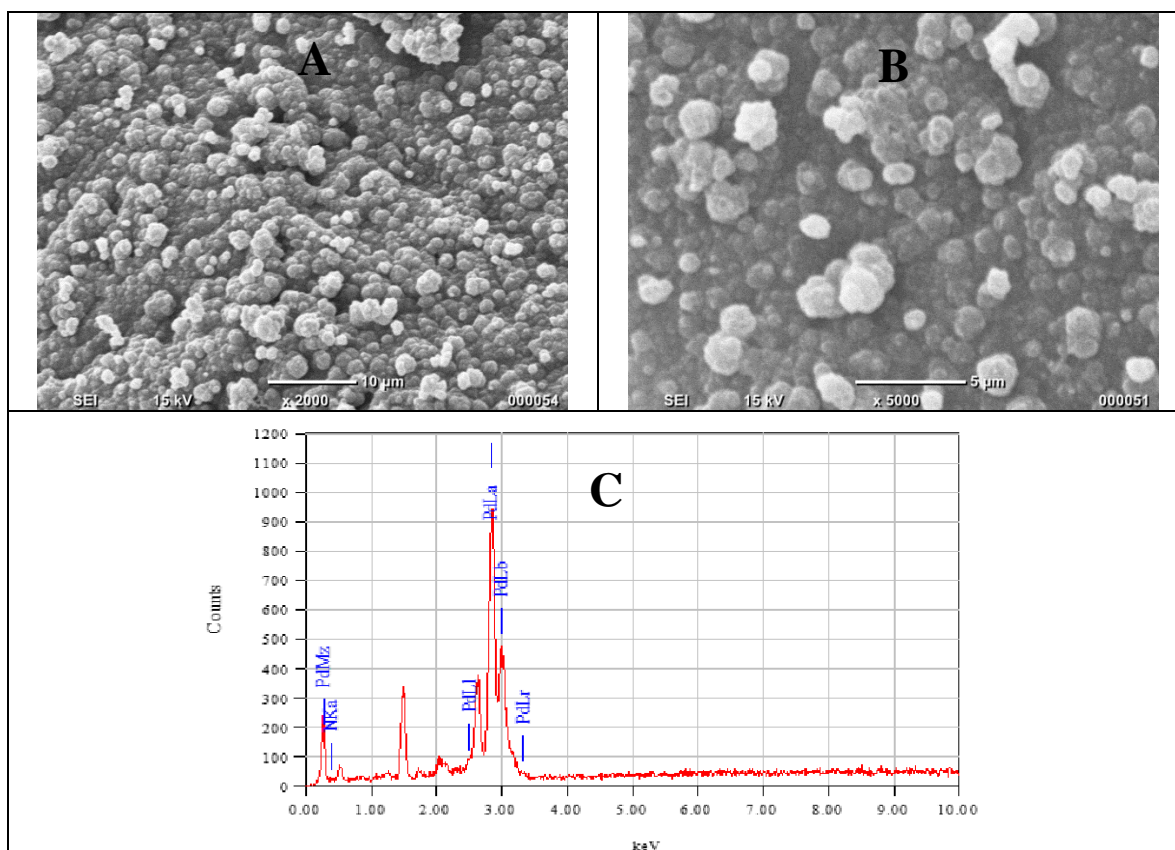


Figure 7. SEM images of the poly(ANI-co-PY)/Pd composite with a magnification of (A) 2000 \times and (B) 5000 \times ; and (C) EDXA spectrum of the composite.

4. CONCLUSION

- Poly(ANI-co-PY)/Pd composite shows enhanced electrocatalytic activity toward hydrazine oxidation compared to PANI/Pd and PPY/Pd composites.
- The optimum operating pH of the copolymer composite for hydrazine oxidation is 6.
- Kinetics study suggests a diffusion-controlled process with a diffusion coefficient value of $1.94 \times 10^{-4} \text{ cm}^2 \text{ s}^{-1}$.
- A calibration curve was obtained with two linear ranges from 3 mM to 0.01 M and from 0.03 M to 0.1 M with an LOD of 0.38 μM , calculated from the lower range.
- The proposed sensor shows high stability, a decrease in I_p of about 20 μA after a test time of five days, and acceptable reproducibility; the standard deviation value of the oxidation peak currents are 3.06%.
- The copolymer/Pd composite performance is affected, to a small extent, by the presence of interfering ions such as NO_3^- and NH_4^+ .

ACKNOWLEDGEMENTS

The authors are grateful to the Scientific Research Dean of Taibah University for supporting this research, project no. 6875/436.

References

1. H. Shirakawa, E. L. Louis, A. G. MacDiarmid, C. K. Chiang and A. J. Heeger, *J. Chem. Soc. Chem. Commun.*, 16 (1977) 578.
2. C. K. Chiang, C. R. Fincher, Y. W. Park, A. J. Heeger, H. Shirakawa, E. J. Louis, S. C. Gau and A. G. MacDiarmid, *Phys. Rev. Lett.*, 40 (1978) 1472.
3. H. Lin, J. Yang, J. Liu, Y. Huang, J. Xiao and X. Zhanga, *Electrochim. Acta*, 90 (2013) 382.
4. J. W. Sobczak, A. Kosinski, A. Bilinski and W. Palczewska, *Adv. Mater. Optics Electro.*, 8 (1998) 295.
5. A. Drelinkiewicz, M. Hasik and M. Choczynski, *Mater. Res. Bull.*, 33 (1998) 739.
6. A. Galal, N. F. Atta, S. A. Darwish and S. M. Ali, *Top. Catal.*, 47 (2008) 73.
7. S. Ghosh, A. Teillout, D. Floresyona, P. Oliveira, A. Hagege and H. Remita, *Inter. J. Hydrogen Energ.*, 40 (2015) 4951.
8. T. Bortolotto, S. E. Facchinetto, S. G. Trindade, A. Ossig, C. L. Petzhold, J. Vargas, O. E. D. Rodrigues, C. Giacomelli and V. Schmidt, *J. Colloid Interf. Sci.*, 439 (2015) 154.
9. E. Lee, M. S. Ahmed, J. You, S. K. Kim and S. Jeon, *Thin Solid Films*, 520 (2012) 6664.
10. N. Kumar, Rosy and R. N. Goyal, *Electrochim. Acta*, 211 (2016) 18.
11. A. McConville and J. Davis, *Electrochem. Commun.*, 72 (2016) 162.
12. Y. Li, D. Deng, X. Xing, N. Chen, X. Liu, X. Xiao and Y. Wang, *Sensor. Actuat. B*, 237 (2016) 133.
13. T. Y. Tekbasoglu, T. Soganci, M. Ak, A. Koca and M. K. Sener, *Biosens. Bioelectron.*, 87 (2017) 81.
14. D. Steinhoff and U. Mohr, *Exp. Pathol.*, 33 (1988) 133.
15. K. Yamada, K. Yasuda, N. Fujiwara, Z. Siroma, H. Tanaka, Y. Miyazaki and T. Kobayashi, *Electrochem. Commun.*, 5 (2003) 892.

16. S. Garrod, M. E. Bollard, A. W. Nicholls, S. C. Connor, J. Connelly, J. K. Nicholson, *Chem. Res. Toxicol.*, 18 (2005) 115.
17. Y. Liang, Y. Zhou, J. Ma, J. Zhao, Y. Chena, Y. Tanga and T. Lu, *Appl. Catal. B*, 103 (2011) 388.
18. L. Chen, G. Hu, G. Zou, S. Shao and X. Wang, *Electrochem. Commun.*, 11 (2009) 504.
19. D. Gioia and I. G. Casella, *Sens. Actuat. B: Chem.*, 237 (2016) 400.
20. X. Chen, W. Liu, L. Tang, J. Wang, H. Pan and M. Du, *Mater. Sci. Eng. C*, 34 (2014) 304.
21. T. Rebis, M. Sobkowiak and G. Milczarek, *J. Electroanal. Chem.*, 780 (2016) 257.
22. S. H. Kazemi, B. Hosseinzadeh and S. Zakav, *Sens. Actuat. B*, 210 (2015) 343.
23. H. Lin, J. Yang, J. Liu, Y. Huang, J. Xiao and X. Zhang, *Electrochim. Acta*, 90 (2013) 382.
24. Y. Gu and W. Wong, *Langmuir*, 22 (2006) 11447.
25. G. Milczarek, *Langmuir*, 25 (2009) 10345.
26. R. Devasenathipathy, V. Mani, S. M. Chen, D. Arulraj and V. Vasantha, *Electrochim. Acta*, 135 (2014) 260.
27. G. Wang, C. Zhang, X. He, Z. Li, X. Zhang and L. Wang, *Electrochim. Acta*, 55 (2010) 7204.
28. S. Daemi, A. A. Ashkarran, A. Bahari and S. Ghasemi, *Sens. Actuat. B*, (2017) In press.
29. A. J. Bard and L. R. Faulkner, *Electrochemical Methods: Fundamentals and Applications*, Wiley, (2001) New York, USA.
30. N. F. Atta, R. A. Ahmed, H. M. A. Amin and A. Galal, *Electroanal.*, 24 (2012) 1.
31. V. Lyutov and V. Tsakova, *J. Electroanal. Chem.*, 661 (2011) 186.
32. S. Ivanov, U. Lange, V. Tsakova and V. M. Mirsky, *Sens. Actuat. B*, 150 (2010) 271.
33. S. K. Kim, Y. N. Jeong, M. S. Ahmed and S. Jeon, *Sens. Actuat. B*, 153 (2011) 246.
34. J. Panchompoo, L. Aldous, C. Downing, A. Crossley and R. G. Compton, *Electroanal.*, 23 (2011) 1568.
35. X. Bo, J. Bai, J. Ju and L. Guo, *Anal. Chim. Acta*, 675 (2010) 29.
36. H. Zhang, J. Huang, H. Hou and T. You, *Electroanal.*, 21 (2009) 1869.
37. N. Maleki, A. Safavi, E. Farjami and F. Tajabadi, *Anal. Chim. Acta*, 611 (2008) 151.
38. B. Haghghi, H. Hamidi, S. Bozorgzadeh, *Anal. Bioanal. Chem.* 398 (2010) 1411.
39. X. Dai, G. G. Wildgoose, R. G. Compton, *Analyst* 131 (2006) 1241.
40. Y. Liu, S. Chen, A. Wang, J. Feng, X. Wu, X. Weng, *Electrochim. Acta*, 195 (2016) 68.
41. G. W. Watt and J. D. Chrisp, *Anal. Chem.*, 24 (1952) 2006.
42. S. Singal, A. K. Srivastava and Rajesh, *Nano-Micro Lett.* 9 (2017) 7.